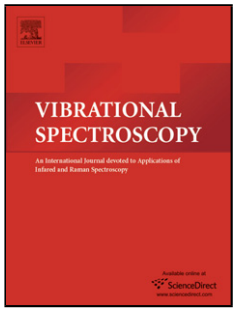

Title: Synthesis, spectroscopic and theoretical studies of (R/S)-piperidinium-3-carboxylic acid 2,6-dichloro-4-nitrophenolate

Author: Michalina Anioła Zofia Dega-Szafran Andrzej Katrusiak Anna Komasa Mirosław Szafran

PII: S0924-2031(16)30003-0
DOI: http://dx.doi.org/doi:10.1016/j.vibspec.2016.01.003
Reference: VIBSPE 2484

To appear in: *VIBSPE*

Received date: 16-7-2015
Revised date: 12-1-2016
Accepted date: 12-1-2016

Please cite this article as: Michalina Aniola, Zofia Dega-Szafran, Andrzej Katrusiak, Anna Komasa, Miroslaw Szafran, Synthesis, spectroscopic and theoretical studies of (R/S)-piperidinium-3-carboxylic acid 2,6-dichloro-4-nitrophenolate, Vibrational Spectroscopy http://dx.doi.org/10.1016/j.vibspec.2016.01.003

Synthesis, spectroscopic and theoretical studies of (R/S)-piperidinium-3-carboxylic acid 2,6-dichloro-4-nitrophenolate

Michalina Anioła, Zofia Dega-Szafran,* Andrzej Katrusiak, Anna Komasa, Mirosław Szafran

Faculty of Chemistry, Adam Mickiewicz University, Umultowska 89b, 61-614 Poznań, Poland

* *Corresponding author*: Tel.: +48 61 8291714; fax: +48 61 8291555
E-mail address: degasz@amu.edu.pl (Z. Dega-Szafran)

HIGHLIGHTS

- Piperidine-3-carboxylic acid and 2,6-dichloro-4-nitrophenol form a PT-complex.
- Complexes are joined into a centrosymmetric dimer, $R^4_4(28)$.
- Dimers are linked into a ladder type cyclamer, $R^4_4(28)$-$R^4_4(20)$-$R^4_4(28)$.
- Structures of monomer, dimer and cyclamer are optimized by B3LYP approaches.
- Experimental Raman, FTIR, second derivative andcalculated IR spectra are compared.

ABSTRACT

(*R*/*S*)-Piperidine-3-carboxylic acid (P3C, nipecotic acid) forms a stable 1:1 hydrogen-bonded complex with 2,6-dichloro-4-nitrophenol (DCNP). Both, in crystal and in the optimized theoretically structure by the B3LYP/6-311++G(d,p) approach the proton is transferred from DCNP to P3C. The (*R*) and (*S*)-stereoisomers complexes of piperidinium-3-carboxylic acid 2,6-dichloro-4-nitrophenolate, $P3C^+H{\cdot}DCNP^-$, aggregate into centrosymmetric cyclic dimers through the $COOH\cdots O^-$ and $N^+H\cdots ONO$ hydrogen bonds of 2.57(1) and 3.06(1) Å, respectively, which in turn are linked into a ladder-type cyclamer through the C-H···Cl hydrogen bonds of 3.71(1) Å. The title compound is characterized by single-crystal X-ray analysis, Raman and FTIR spectroscopies. The structures of the complexes of the ratio 1:1 (monomer), 2:2 (dimer) and 4:4 (cyclamer) of $P3C^+H{\cdot}DCNP^-$ units are optimized by the B3LYP/6-311++G(d,p) approach and compared with the solid state experimental structure. Detail interpretation of the vibrational spectra has been carried out by computing Potential

Energy Distribution (PED). Charge delocalization has been analyzed using the Natural Bond Orbital (NBO) method.

Keywords: Nipecotic acid; 2,6-dinitro-4-nitrophenol; X-ray diffraction; Raman and FTIR spectra; DFT calculations; Hydrogen bonds.

1. Introduction

Hydrogen bonding is one of the most import non-covalent chemical interactions. The proton-transfer reaction plays an import role in various chemical and biological processes such as stabilization of bio-molecular structure [1], control of the rate of enzymatic reaction, [2], as well as the formation of supramolecular structures [3]. Complexes of phenols with nitrogen and oxygen bases belong to the most frequently investigated hydrogen-bonded and proton-transfer systems in the solution [4-11], crystal [12,13] and in gas phase [14,15]. The proton-transfer reaction in such systems strongly depends on the acidity of phenol. By changing the type and number of substituents in the phenol ring one can regulate almost continuously the pK_a value [16,17]. 2,6-Dichloro-4-nitrophenol (DCNP) with the pK_a of 3.70 value, is one of the most acidic phenols and it easily forms crystalline complexes with different bases. A great number of complexes of DCNP with pyridines [5,18-24], pyridine N-oxides [25,26], betaines [27-30] and piperidine acetic acid [31] have been investigated by spectroscopic methods as well as by X-ray diffraction. The strength and length of N-H···O and O-H···O hydrogen bonds strongly depend on the proton-acceptor properties of bases.

The aim of this work is to study the molecular structure of piperidine-3-carboxylic acid (nipecotic acid) with 2,6-dichloro-4-nitrophenol, P3C·DCNP (**1**). The P3C is a zwitterionic β-amino acid with the chiral center at C(3) (Fig. 1). The energy and structures of several stable piperidine-3-carboxylic acid tautomers have been calculated by the B3LYP/6-311++G(d,p) approach [32], and it was found that the most stable structure of P3C exists in a zwitterionic

form, which is stabilized by an intramolecular N-H···O hydrogen bond. In the crystal of P3C the carboxylic group is in the equatorial position [33]. A similar conformation has been observed in its hydrogen-bonded complexes of P3C with hydrochloric acid [34], L-tartaric acid [35] and squaric acid [36]. However, in the complexes of P3C with *p*-hydroxybenzoic acid [37] and salicylic acid [38], the carboxylate group is in the axial position. P3C as a zwitterion has two interacting centers, the proton-donor N^+H_2 group and the proton-acceptor COO^- group with the pK_a values of 10.20 and 3.45, respectively [39]. The new P3C·DCNP compound (**1**) is characterized by single-crystal X-ray analysis (Figs. 1 and 2), Raman and FTIR spectroscopies. The ^1H and ^{13}C NMR chemical shifts characterizing the novel compound are given in the Experimental Section. The structures of the P3C·DCNP in the stoichiometry 1:1 (**2-M** monomer) and 2:2 (**2-D** dimer) are optimized at the B3LYP/6-311++G(d,p) level of theory and that at the ratio 4:4 (**2-C** cyclamer) at the B3LYP/6-31G(d,p) level of theory (Fig. 3).

2. Experimental and calculations

To 0.838 g (0.0065 M) of piperidine-3-carboxylic acid in the methanol-water (5:1) solution (6 ml), 1.349 g (0.0065 M) of 2,6-dichloro-4-nitrophenol dissolved in 2 ml of methanol was added and the reaction mixture was heated for 5 min. The solvents were evaporated and the crude product was recrystallized from the mixture of ethanol-acetonitrile (2:1) The 1:1 complex of piperidine-3-carboxylic acid with 2,6-dichloro-4-nitrophenol (**1**) melts at 176 ^oC. Elemental analysis calculated for $C_{12}H_{14}N_2O_5Cl_2$: %C, 42.75; %H, 4.19; %N, 8.31; found: %C, 42.71; %H, 4.16; %N, 8.33. NMR spectra (ppm) in DMSO-d_6: δ^1H: H(2A) 2.98, H(2E) 3.36, H(3A) 2.69, H(4A) 1.63, H(4E) 1.99, H(5A) 1.63, H(5E) 1.78, H(6A) 2.80, H(6E) 3.19, H(13,15) 8.05; $\delta^{13}C$: C(2) 44.04, C(3) 37.95, C(4) 24.77, C(5) 21.15, C(6) 43.11, C(7) 173.25, C(11) 163.52, C(12,16) 122.67, C(13,15) 124.46, C(14) 130.60 are

shown in Fig. S1 (Supplementary material). Letters A and E denote the axial or equatorial positions of H-atoms.

FTIR spectra were measured in Nujol and Fluorolube suspensions between KBr plates using a Bruker IFS 66v/S instrument, with the resolution of 2 cm^{-1}. Each spectrum was accumulated by acquisition of 64 scans. The FTIR spectrum presented was obtained with the use of the split mull technique, which combines the spectra recorded in two ranges, in the range of 4000-1325 cm^{-1} from the spectrum measured in Fluorolube and in the range of 1325-400 cm^{-1} from the spectrum measured in Nujol. The Raman spectrum of crystalline sample was measured on a Bruker FRA-106/S instrument operating at the 1064 nm exciting line of Nd:YAG laser with the resolution of 1 cm^{-1}. The spectrum was accumulated by acquisition of 200 scans. The NMR spectra were recorded on a Varian VNMRS-400 spectrometer operating at 402.64 and 101.24 MHz for ^{1}H and ^{13}C, respectively. The spectra were measured in DMSO-d_6 relative to an internal standard of TMS. Elemental analysis was made using an Elemental Model Vario EL III.

X-Ray diffraction data of the 1:1 complex of P3C with DCNP (**1**) were collected on a KUMA KM-4 CCD diffractometer [40,41]. The structure was solved by direct methods using SHELXS-97 and refined on F^2 by the full-matrix least-squares with SHELXL-97 [42]. The crystal data, details of data collection and structure refinement are given in Table 1 and the final atomic coordinates in Table S1 (Supplementary material). The crystallographic and structural data in CIF format are available from the Cambridge Crystallographic Database Centre (CCDC 1062233).

The DFT calculations were performed with the GAUSSIAN 09 program package [43]. The calculations employed the B3LYP exchange-correlation functional, which combines the hybrid exchange functional of Becke [44,45] with the gradient-correlation functional of Lee et al. [46] and the split-valence polarized 6-311++G(d,p) and 6-31G(d,p) basis sets [47]. The X-

ray geometry of **1** was used as a starting point for the calculations. The natural bond orbital (NBO) [48] calculations were performed using the Gaussian 09 package at the B3BLYP/6-311++G(d,p) level of theory. The calculated IR frequencies are positive and confirmed that the optimized structures were in the states of minimum energy. The Potential Energy Distribution (PED) of the vibrational modes of the optimized molecules (2-**D**) was determined using VEDA 4 program [49,50]. Only the PED greater than 10% were considered. The symmetry coordinates (S_n) and their descriptions are given in Table S2 in Supplementary information.

3. **Results and discussion**

3.1. Crystal structure

(*R*/*S*)-piperidine-3-carboxylic acid (P3C) forms a stable co-crystalline complex (**1**) at the 1:1 ratio with 2,6-dichloro-4-nitrophenol (DCNP). The labeling of atoms is shown in Fig. 1. The bond lengths, bond and torsion angles are given in Table 2. The proton from DCNP is transferred to P3C, generating piperidinium-3-carboxylic acid cation, $P3C^{+}H$, and 2,6-dichloro-4-nitrophenolate anion, $DCNP^{-}$. P3C exists in the zwitterionic form in the solid state [33] hence, the proton from the phenolic OH group is transferred to the carboxylate group of P3C, which it is a proton-acceptor. In the crystalline state the protonated (*R*)- and (*S*)-$P3C^{+}H$ cations and two deprotonated $DCNP^{-}$ anions form a centrosymmetric cyclic dimer through the O(1)-H(1)···O(13) and N(1)-H(2N)···O(15) hydrogen bonds of 2.57(1) and 3.06(1) Å, respectively (Fig. 1, Table 3). The graph descriptor of the dimer is $R^4_4(28)$ [51] (Fig. 1). In this graph descriptor *R* indicates the ring aggregate, with the smallest number of atoms along the ring, and four H-donors and four H-acceptors are involved. Complex **1** is triclinic of space group $P\bar{1}$ with one such dimer in the unit cell. The dimer is bridged with the neighboring one through the weak C(2)-H(2A)···Cl(2) intermolecular contacts of 3.71(1) Å forming an

additional ring described by graph $R^4_4(20)$ [51] (Fig. 2, Table 3). Such network of the hydrogen bonds can be classified as a ladder type supramolecule [52].

The piperidinium ring in the P3C$^+$H cation has a slightly flattened chair conformation with the carboxylic group in the axial position. The mean endocyclic torsion angle is 55.7^o (Table 2). The axial position of the COOH group implies a preference to form a cyclic form. The carboxylic O-H group has a *cis* orientation. The C(7)-O(1) bond length of 1.309(4) Å, and the C(7)-O(2) bond length of 1.201(4) Å is consistent with the protonation side at the O(1) atom. The O(2) oxygen atom is only involved in the C(6)-H(6A)···O(2) contacts of 3.42(1) Å (Table 3), which can be treated as a weak hydrogen bond [53].

3.2. Optimized structures

Four models of P3C with DCNP complexes (**2)** were optimized at the B3LYP/6-311++G(d,p) and B3LYP/6-31G(d,p) levels of theory. The P3C$^+$H·DCNP$^-$ unit is treated as a monomer of the stoichiometry P3C to DCNP 1:1 and it is denoted by **2-M*a***, **2-M*b*** (M - as monomer). The complex (P3C$^+$H·DCNP$^-$)$_2$ of the 2:2 ratio is treated as a dimer **2-D** (D - as dimer) and (P3C$^+$H·DCNP$^-$)$_4$ of the 4:4 ratio as a cyclamer, **2-C** (C as cyclamer). Their optimized structures are shown in Fig. 3. The calculated bond lengths, bond and torsion angles are listed in Table 2. The total energy of **2-M*a*** is -1871.985138 a.u., of **2-M*b*** is –1871.970247 a.u., of **2-D** is -3743.997915 a.u. and of **2-C** is –7485.376015 a.u. The stability increases in the order **2-M*b*** < **2-M*a*** < **2-D** < **2-C**.

The **2-M*a*** is neutral. The carboxylic proton O(1)-H of P3C assumes the *trans* orientation and forms an intramolecular hydrogen bond to the tertiary nitrogen atom, N(1), of 2.668 Å (Table 3). The P3C components in the complex **2**-M***a*** has a structure similar to that of the most stable tautomer in P3C itself [32]. The DCNP molecule is connected to P3C by O(13)-

H(5)···O(1) hydrogen bond involving the hydroxy group of DCNP and carboxylate group of P3C with the O···O distance of 2.761 Å (Fig. 3, Table 3).

In the second optimized 1:1 complex, **2-M*b***, the $P3C^{+}H$ and $DCNP^{-}$ ions are linked through $N^{+}H\cdots O(15)$ hydrogen bond of 2.600 Å, formed between the ammonium group of $P3C^{+}H$ cation and nitro group of $DCNP^{-}$ anion. The energy of **2-M*b*** is by 39.1 $kJ\cdot mol^{-1}$ higher than that of **2-M*a***. A similar interaction between the amino group and nitro group of DCNP was suggested by Al-Ahmary et al. for the 2:1 complex of 4-aminopyridine with DCNP in solution [11].

In the 2:2 complex, **2-D**, similarly as in the crystal of **1**, phenolic proton H(1) is transferred to piperidine-3-carboxylic acid. Two stereoisomeric molecules (*R*)- and (*S*)-$P3C^{+}H\cdot DCNP^{-}$ (denoted as I and II, Fig. 3) are joined into a cyclic **2-D**. The molecules are linked through two O(1)-H···O(13) and two N(1)-H···O(15) hydrogen bonds of 2.541 and 2.773 Å, respectively (Table 3). The optimized structure **2-D** is almost symmetric with the calculated dipole moment of 0.004 D.

The optimized 4:4 structure of **2-C** is significantly asymmetric and the calculated dipole moment is 1.72 D. Four molecules of $P3C^{+}H\cdot DCNP^{-}$, denoted as I-IV (Fig. 3), form a three cyclic ring system, which are linked through the O(1)-H···O(13), N(1)-H···O(15) and C(2)-H···Cl(2) hydrogen bonds. The O(1)···O(13) distances vary from 2.490 to 2.521 Å, N(1)-H···O(15) from 2.769 to 2.889 Å and C(2)-H···Cl(2) are 3.861 and 3.801 Å (Table 3).

For comparison, the structures of pure components, P3C and DCNP were optimized by the B3LYP/6-311++G(d,p) approach. The calculated energy and dipole moment of P3C (in the axial conformation of the carboxylic group) are E = -440.612945 a.u. and μ = 6.51 D, and those of DCNP are E = -1431.361037 a.u. and μ = 3.96 D. Their optimized structures are shown in Fig. S2, while their geometrical parameters are given in Tabless S3 and S4 (Supplementary material). The main difference in the geometrical parameters between the

calculated complexes of **2** and pure DCNP is the C(11)-O(13) bond length, which is much longer in DCNP moiety (1.333 Å) in **2-M*a***, than in DCNP$^-$ anion (1.223 – 1.289 Å) in **2-M*b***, **2-D** and **2-C.**

There are some deviations of the geometrical parameters between the crystal structure of **1** and optimized structure **2-D**, which stem from the fact that the X-ray data refer to the molecules in the chemical environment while the calculated data refer to the isolated molecules.

The natural bond orbital (NBO) analysis have proved to be an effective tool for chemical interpretation of electron density. It gives information about interactions between electron-donors and electron-acceptors. It is also an efficient method for studying intra- and intermolecular bonding and interaction among bonds [48,54-57]. Table 4 summarizes the natural atomic charges of atoms in **2-M*a***, **2-M*b***, **2-D** and pure components of the complexes, P3C and DCNP. The magnitude of the charge nitrogen N(1) atom is more negative in **2-M*a*** and P3C than in the other models, which suggest the presence of the neutral form of P3C unit in **2-M*a***. This neutral form of P3C unit in **2-M*a*** is confirmed also by the charge H(1N) atom, which is less positive in **2-M*a*** and P3C, where this atom is not hydrogen-bonded, as in **2-M*b*** and **2-D**. The more negative charge O(1) atom than O(2) one in all optimized structures confirms the presence of the carboxylic group and a proton-transfer from DCNP to P3C in **2-M*b*** and **2-D**. The charges C(7) atoms are positive and of similar values (0.81 *e*). The H(1) atom engaged in the O-H···O hydrogen bond in **2-D** is characterized by the more positive charge than that in the other models. The charges C(11) atom, which are more positive in **2-M*b*** and **2-D** (0.4 *e*) than in **2-M*a*** and DCNP (0.3 *e*) show a difference between the electronic structure of phenol and phenolan.

3.3. The experimental and computed IR spectra

The solid-state experimental Raman and FTIR spectra of piperidinium-3-carboxylic acid 2,6-dichloro-4-nitrophenolate (**1**) in the range of 3600-400 cm^{-1} is shown in Figs. 4a and c, respectively. The distribution of the vibrational energy in internal coordinates (PED) (Table S2), defined and recommended by Keresztury and Jalsovszky [58], was used to assign vibrational bands in **2-D** (Table 5). Two $P3C^{+}H{\cdot}DCNP^{-}$ units in **2-D** are denoted as (I) and (II) (Fig. 3). The calculated IR spectrum (scaled) of **2-D** in the Lorentzian band shapes is shown in Fig. 4d. Generally, theoretical calculations overestimate the magnitudes of vibrational frequencies. These discrepancies can be corrected by scaling the calculated wavenumbers with a proper factor [59,60] or by scaling the equation [61,62]. The vibrational frequencies are scaled by the precomputed vibrational scaling factor 0.967, recommended for the B3LYP/6-311++G(d,p) calculations [60] and are collected as ν_{scaled} (Table 5). Although the structure of the optimized **D-2**, is almost symmetrical (μ = 0.004 D), from the theoretical point of view a number of (*3n-6*) 204 bands are calculated. The frequencies of the most vibrations are duplicated, however, one of the band is much more intensive than the other ones. They intensities vary between 6763 to 0.0001 $km{\cdot}mol^{-1}$. The bands of intensities below 1 $km{\cdot}mol^{-1}$ are neglected. The wavenumbers of the experimental (ν_{exp}), calculated (ν_{calc}) and scaled (ν_{scaled}) bands are listed in Table 5.

As X-ray analysis shown, there are three different medium-strong hydrogen bonds linking ions of $P3C^{+}H{\cdot}DCNP^{-}$ into 2:2 and 4:4 complexes, $O\text{-}H\cdots O^{-}$, $N^{+}H_2\cdots O_2N$ and $C\text{-}H\cdots Cl$, which cause a broadening of the absorption band in the 3500-2000 cm^{-1} region. The bands at 2853 and 2570 cm^{-1} are attributed to the $\nu N^{+}H\cdots O$ and $\nu O\text{-}H\cdots O^{-}$ modes, similarly as in the spectrum of P3C, in which the broad band attributed to the $\nu N\text{-}H\cdots O$ vibration appears at ca. 2600 cm^{-1} (Fig. S3) [32], however, the νOH mode of the phenolic group in the

spectrum of DCNP gives a band at 3383 cm^{-1} (Fig. S4) [63,64]. The spectra of pure components, P3C and DCNP, are plotted in Fig. 4c, as a long-dashed red line and short-dashed blue one, respectively (see also the experimental Raman, FTIR and computed (scaled) IR spectra of P3C and DCNP components in Figs. S3 and S4). The broad band with sub-structure overlaps the stretching vibrations of CH_2 and CH bands in the 3100-2900 cm^{-1} range in the FTIR spectrum of **1** (Fig. 4c). This broad absorption is absent both in the Raman spectrum (Fig. 4a) and in the second derivative spectrum, d^2 (Fig. 4b), because in the Raman spectrum the intensity of the O-H stretching vibration is usually weak [65], while in the second-derivative spectrum, d^2, the relative amplitude of the negative bands varies inversely to the square of their half-width ratio [66,67], hence the broad bands in the FTIR spectrum are not observed in d^2. The minima in the d^2 spectrum have the same wavenumbers as the maxima in the absorbance spectra. The d^2 spectrum is shown in Fig. 4b and the wavenumbers of minima are listed in Table 5 as νd^2. The computed wavenumbers of $\nu_{as}NH_2$ and ν_sNH_2 are predicted at 3214 and 3313 cm^{-1}, and of νNH···O at 2876 and 2874 cm^{-1}, while νOH···O at 2714 cm^{-1} (Table 5, Fig. 4d), and they show a rather good agreement with the experimental observation, although, the experimental spectra refer to the molecule in the chemical environment, whereas the computed spectra to the isolated molecule. The NH in-plane deformation modes are observed in the FTIR spectrum of **1** at 1679 and 1474 cm^{-1}, similarly as in the IR spectrum of P3C [32], in which they are at 1570 and 1484 cm^{-1} (Fig. S3b). Both bands are inactive in the Raman spectrum (Figs. 4a, S3a). In the theoretical spectrum of **2-D,** the δNH modes are predicted at 1626 and 1474 cm^{-1}, however, the intensity of the last one is very low (Fig. 4d). The OH in-plane deformation mode is observed in the FTIR spectrum of **1** at 1421 cm^{-1}, while the OH out-of-plane deformation vibration at 921 cm^{-1}, whereas they are predicted by DFT calculation at 1415 and 991 cm^{-1}, respectively.

In the FTIR spectrum the νCH and νCH_2 are overlapped by the broad absorption in the 3500-2000 cm^{-1} region, however they are well resolved in the Raman spectrum, although they are of less intense (Fig. 4a). They can also be easily distinguished in the second-derivative spectrum, d^2 (Fig. 4b). The experimental CH stretching vibrations of C(13)H and C(15)H at 3108 cm^{-1} are predicted by the DFT calculation at 3124 and 3121 cm^{-1}, while νC(3)H is predicted at lower frequencies, at 2981 cm^{-1}. The νCH_2 vibrations of the piperidine ring appear at 3077, 3018, 3004, 2977, 2951, 2935 and 2913 cm^{-1} in the Raman spectrum, similarly as in the FTIR spectrum of P3C itself (Fig. S3d) [32]. Theoretically, twelve wavenumbers are predicted for the asymmetric and symmetric νCH_2 vibrations. The bending modes of methylene groups are predicted to give bands in the region 1466-1149 cm^{-1}. These modes are also mixed with the contributions of CC, CN, CO stretching and bending vibrations in this region (Table 5).

The CO stretching band of low intensity appears at 1706 cm^{-1}, similarly as in the FTIR spectra of the complexes of P3C with L-tartaric acid at 1703 cm^{-1} [35] and with squaric acid at 1733 cm^{-1} [36], in which P3C is an acceptor of proton. In the complexes of P3C without a proton transfer, with salicylic acid and p-hydroxybenzoic acid, the $\nu_{as}COO$ bands are observed at 1610 and 1608 cm^{-1}, respectively [37,38]. The computed position of this band in the IR spectrum of **2-D** is at 1744 cm^{-1}. This wavenumber suggests that COOH group is present in the complex investigated, which is consistent with the protonation process by the proton transfer from DCNP to the carboxylate group of P3C. In the FTIR spectrum of P3C, which exists in the zwitterionic form in the solid state, the $\nu_{as}COO$ mode at 1632 cm^{-1} is observed (Fig S3) [32], while it is predicted at 1755 cm^{-1}, for the neutral form of P3C. The band assigned to $\nu_s CO$ is observed at 1220 cm^{-1} in the spectrum of **1** and it is predicted by computation at 1188 cm^{-1} in the spectrum of **2-D**.

The νC=C vibrations in the aromatic ring of DCNP unit in the FTIR spectrum of **1** give bands in the range typical of benzene derivatives 1625-1475 cm^{-1} [68,69]. The theoretically predicted νC=C mode of the aromatic ring are at 1563, 1492. 1451 cm^{-1}, of νC-O mode at 1538, the mode of νC-NO_2 is predicted at 1344, 1273 and 1122 cm^{-1}. However the theoretically computed νC=C in pure DCNP are assigned as a band of strong intensity at 1562, 1527 cm^{-1} and of a low intensity at 1442 cm^{-1} (Fig. S4).

The bands at 1376, 1279, 1119, and 719 cm^{-1} are attributed to the $\nu_{as}NO_2$, ν_sNO_2, δNO_2 and γNO_2 in the experimental spectrum of **1**, whereas the corresponding theoretical bands are predicted at 1374, 1344, 1273, 1122 and 716 cm^{-1}, similarly to those found in the spectra of complexes of dimethylphenylbetaine with DCNP [30]. In the FTIR spectrum of DCNP the $\nu_{as}NO_2$ and ν_sNO_2 are observed at 1531 and 1233 cm^{-1},while the theoretically predicted positions are at 1527 and 1317 cm^{-1}, respectively (Fig. S4). In the experimental spectrum of **1** **t**he band at 752 cm^{-1} is attributed to the C-Cl modes, while they are theoretically predicted at 888 and 759 cm^{-1}, and appear in a typical range of C-Cl modes [68], whereas in the spectrum of DCNP the νC-Cl band is observed at 811 cm^{-1} and predicted at 765 cm^{-1}.

The infrared spectra of complexes of the stoichiometry 1:1 (**2-M*a*** and **2-M*b***), 2:2 (**2-D**) and 4:4 (**2-C**) calculated and scaled, by a factor of 0.967 (for 1:1 and 2:2 complexes) and 0.961 (for 4:4), are shown in stocked plots in Fig. 5. The bands assigned to the O(11)H and O(1)H stretching vibrations in the **2-M*a*** spectrum are predicted at 3572 and 2930 cm^{-1}, respectively, and suggest that OH groups are not engaged in strong hydrogen bonds. However, in the IR spectrum of **2-M*b***, the free νO(1)H and νN(1)H(2N) vibrations are predicted to be at 3621 and 3342 cm^{-1}, respectively, while the band due to νN(1)H(1N)···O(15) at 2113 cm^{-1} corresponds to the interaction between the amino group and nitro group. It is shifted to the lower wavenumbers in a comparison to those in the spectra of **2-D** and **2-C** (Fig. 5c and Fig. 5d). This fact can be explained by much shorter N(1)···O(15)

distance in **2-M*b*** than in **2-D** and **2-C** (Table 3). The ν_{as}COO modes are theoretically predicted at 1765, 1763, 1744 and 1665 cm^{-1} in the spectra of **2-M*a***, **2-M*b***, **2-D** and **2-C**, respectively, which suggest that the carboxylic groups are present in all models. The proposed assignments of bands in the calculated spectra are made using the Gauss-View molecular visualization program [70].

4. Conclusions

Racemic (*R*/*S*)-piperidine-3-carboxylic acid (P3C, nipecotic acid) forms with 2,6-dichloro-4-nitrophenol (DCNP) a centrosymmetric dimer (2:2 complex), built of (*R*) and (*S*) stereoisomers of piperidinium-3-carboxylic acid cations and 2,6-dichloro-4-nitrophenolate anions, described by graph $R^4_4(28)$. The 2:2 complex are further linked into a ladder-type structure through the attraction between proton of the piperidinium ring and chlorine atom of phenol. Hence, fused cyclamers are formed of three rings, described by the graphs $R^4_4(28)$-$R^4_4(20)$-$R^4_4(28)$. The solid-state FTIR spectrum shows a broad absorption in the 3500-2000 cm^{-1} region attributed to the COOH···O, and N^+-H···ONO hydrogen bonds of 2.57(1) and 3.06(1) Å, respectively, which is absent in the Raman spectrum and IR-second derivative spectrum (d^2). A comparison of the νCO vibrations in the spectrum of the complex investigated with the spectrum of pure P3C shows, that the proton is transferred from DCNP to the carboxylate group in P3C in the complex. The P3C-DCNP complexes as monomer and dimer are optimized at the B3LYP/6-311++G(d,p), and cyclamer at the B3LYP/6-31G(d,p) level of theory. Both IR frequencies in the spectra of the experimental and optimized structures are consistent with geometrical parameters. The NBO analysis confirms the proton-transfer from DCNP to P3C in all optimized structures.

Acknowledgements

The computations were performed at the Poznań Supercomputing and Networking Center and supported in part by PL-Grid Infrastructure.

Appendix A. Supplementary material

Supplementary data (Fig. S1-S4, Tables S1-S4) associated with this article can be found in the online version at http://dx.doi.org/.....

References

[1] S. Deechongkit, H. Nguyen, E.T. Powers, P.E. Dawson, M. Gruebele, J.W. Kelly, Nature 430 (2004) 101-105.

[2] G. Grégoire, C. Jouvet, C. Dedonder, A.L. Sobolewski, Chem. Phys. 324 (2006) 398-404.

[3] Yu.E. Alexeev, B.I. Kharisov, T.C. Hernández-Garcia, A.D. Garnovskii, Coord. Chem. Rev. 254 (2010) 794-831.

[4] B. Brzezinski, B. Brycki, G. Zundel, T. Keil, J. Phys. Chem. 95 (1991) 8598-8600.

[5] B. Brycki, M. Szafran, J. Mol. Liquids, 50 (1994) 83-101.

[6] M. Ilczyszyn, J. Chem. Soc. Faraday Trans. 90 (1994) 1411-1414.

[7] M. Ilczyszyn, H. Ratajczak, J. Chem Soc. Faraday Trans. 91 (1995) 3859-3867.

[8] A. Wakisaka, Y. Yamamoto, Y. Akiyama, H. Takeo, F. Mizukami, K. Sakaguchi, J. Chem. Soc. Faraday Trans. 92 (1996) 3339-3344.

[9] M.M. Habeeb, A.S. Al.-Attas, M.T. Basta, J. Mol. Liquids, 150 (2009) 56-61.

[10] K.M. Al.-Ahmary, M.M. Habeeb, E.A. Al.-Solmy, J. Mol. Liquids, 158 (2011) 161-165.

[11] K.M. Al.-Ahmary, E.A. Al.-Solmy, M.M. Habeeb, Spectrochim. Acta A 126 (2014) 260-269.

[12] I. Majerz, Z. Malarski, L. Sobczyk, Chem. Phys. Lett. 274 (1997) 361-364.

[13] H. Szatyłowicz, T.M. Krygowski, Polish J. Chem. 79 (2004) 1719-1731.

[14] T.M. Krygowski, J.E. Zachara, H. Szatyłowicz, J. Phys. Org. Chem. 17 (2004) 1-5.

[15] M.R. Sameti, Asian J. Chem. 21 (2009) 879-884.

[16] M. Ilczyszyn, Z. Latajka, H. Ratajczak, Org. Magn. Res. 13 (1980) 132-136.

[17] L. Sobczyk, Ber. Bunsenges. Phys. Chem. 102 (1998) 377-383.

[18] I. Majerz, W. Sawka-Dobrowolska, L. Sobczyk, J. Mol. Struct. 297 (1993) 177-184.

[19] I. Majerz, W. Sawka-Dobrowolska, L. Sobczyk, Polish J. Chem. 67 (1993) 1657-1665.

[20] I. Majerz, W. Sawka-Dobrowolska, L. Sobczyk, J. Mol. Struct. 319 (1994) 1-9.

[21] I. Majerz, W. Sawka-Dobrowolska, L. Sobczyk, Acta Phys. Pol. 88 (1995) 349-357.

[22] I. Majerz, W. Sawka-Dobrowolska, L. Sobczyk, J. Mol. Struct. 375 (1996) 37-42.

[23] I. Majerz, W. Sawka-Dobrowolska, J. Chem. Crystallogr. 26 (1996) 147-152.

[24] I. Majerz, W. Sawka-Dobrowolska, L. Sobczyk, J. Mol. Struct. 416 (1997) 113-120.

[25] Z. Dega-Szafran, A. Kania, M. Grundwald-Wyspiańska, M. Szafran, E. Tykarska, J. Mol. Struct. 381 (1996) 107-125.

[26] E. Tykarska, Z. Dega-Szafran, M. Grundwald-Wyspiańska, M. Szafran, Polish J. Chem. 72 (1998) 470-479.

[27] Z. Dega-Szafran, A. Komasa, M. Grundwald-Wyspiańska, M. Szafran, G. Buczak, A. Katrusiak, J. Mol. Struct. 404 (1997) 13-25.

[28] M. Szafran, Z. Dega-Szafran, G. Buczak, A. Katrusiak, M.J. Potrzebowski, A. Komasa, J. Mol. Struct. 416 (1997) 145-160.

[29] Z. Dega-Szafran, E. Sokołowska, J. Mol. Struct. 565-566 (2001) 17-23.

[30] M. Szafran, A. Komasa, K. Ostrowska, A. Katrusiak, Z. Dega-Szafran, Spectrochim Acta A 136 (2015) 1216-1226.

[31] Z. Dega-Szafran, G. Dutkiewicz, Z. Kosturkiewicz, M. Petryna, M. Szafran, J. Mol. Struct. 741 (2005) 115-120.

[32] S. Yurdakul. N.C. Yaşayan, S. Badoğlu, Optics and Spectroscopy 116 (2014) 906-918.

[33] L. Brehm, P. Krosgaard-Larsen, G.A.R. Johnston, K. Schaumburg, Acta Chem. Scand. B 30 (1976) 542-548.

[34] R.S. Narasegowda, H.S. Yathirajan, M. Bolte, Acta Crystallogr. E 61 (2005) o763-o764.

[35] E. Bartoszak-Adamska, Z. Dega-Szafran, M. Jaskólski, M. Szafran, J. Mol. Struct. 999 (2011) 98-105.

[36] E. Bartoszak-Adamska, Z. Dega-Szafran, A. Komasa, M. Szafran, Chem. Phys. 444 (2014) 7-14.

[37] Z. Dega-Szafran, M. Jaskólski, M. Szafran, Polish J. Chem. 81 (2007) 931-946.

[38] E. Bartoszak-Adamska, Z. Dega-Szafran, M. Krociak, M. Jaskólski, M. Szafran, J. Mol. Struct. 920 (2009) 68-74.

[39] R.-S. Tsai, B. Testa, N. El-Tayar, P.-A. Carrupt, J. Chem. Soc. Perkin Trans. 2 (1991) 1797-1802.

[40] KUMA KM4 CCD Software, version 161, 1999, Kuma Diffraction (Wroclaw, Poland).

[41] CrysAlis 162, Kuma Diffraction, 1999 (Wroclaw, Poland).

[42] G.M. Sheldrick, Acta Crystallogr. A 64 (2008) 112-122.

[43] M.J. Frisch, G.W. Trucks, H.B. Schlegel, G.E. Scuseria, M.A. Robb, J.R. Cheeseman, G. Scalmani, V. Barone, B. Mennucci, G.A. Petersson, H. Nakatsuji, M. Caricato, X. Li, H.P. Hratchian, A.F. Izmaylov, J. Bloino, G. Zheng, J.L. Sonnenberg, M. Hada, M. Ehara, K. Toyota, R. Fukuda, J. Hasegawa, M. Ishida, T. Nakajima, Y. Honda, O. Kitao, H. Nakai, T. Vreven, J.A. Montgomery, Jr., J.E. Peralta, F. Ogliaro, M. Bearpark, J.J. Heyd, E. Brothers, K.N. Kudin, V.N. Staroverov, T. Keith, R. Kobayashi, J. Normand, K. Raghavachari, A. Rendell, J.C. Burant, S.S. Iyengar, J. Tomasi, M. Cossi, N. Rega, J.M. Millam, M. Klene, J.E. Knox, J.B. Cross, V. Bakken, C. Adamo, J. Jaramillo, R. Gomperts, R.E. Stratmann, O. Yazyev, A.J. Austin, R. Cammi, C. Pomelli, J.W. Ochterski, R.L. Martin, K. Morokuma, V.G. Zakrzewski, G.A. Voth, P. Salvador, J.J. Dannenberg, S. Dapprich, A.D. Daniels, O. Farkas, J.B. Foresman, J.V. Ortiz, J. Cioslowski, D.J. Fox, GAUSSIAN 09, Revision B.01, Gaussian, Inc., Wallingford CT, 2010.

[44] A.D. Becke, J. Chem. Phys. 98 (1993) 5648-5652.

[45] A.D. Becke, J. Chem. Phys. 107 (1997) 8554-8560.

[46] C. Lee, W. Yang, R.G. Parr, Phys. Rev. B 37 (1988) 785-789.

[47] W.J. Hehre, L. Random, P.V.R. Schleyer, J.A. Pople, Ab Initio Molecular Orbital Theory, Wiley, New York, 1986.

[48] A.E. Reed, L.A. Curtiss, F. Weinhold, Chem. Rev. 88 (1988) 899-926.

[49] M.H. Jamróz, Vibrational Energy Distribution Analysis; VEDA 4 Program, Warsaw, Poland, 2004-2010, http://smmg.pl.

[50] M.H. Jamróz, Spectrochim. Acta A 114 (2013) 220-230.

[51] M.C. Etter, J.C. MacDonald, J. Bernstein, Acta Crystallogr. B 46 (1990) 256-262.

[52] T. Yuge, T. Sakai, N. Kai, I. Hisaki, M. Miyata, N. Tohnai, Chem. Eur. J. 14 (2008) 2984-2993.

[53] G.R. Desiraju, T. Steiner, The weak hydrogen bond in structural chemistry and biology, Oxford University Press, Oxford 2001.

[54] A.E. Reed, F. Weinhold, J. Chem Phys. 78 (1983) 4066-4073.

[55] S. Snehalatha, C. Ravikumar, I. HubertJoe, N. Sekar, V.S. Jayakumar, Spectrochim. Acta A 72 (2009) 654-662.

[56] D.M. Suresh, A. Amalanthan, S. Sebastian, D. Sajan, I. HubertJoe, V. Bena Jothy, I. Nemec, Spectrochim. Acta A 115 (2013) 595-602.

[57] R.P. Gangadharan, S. Sampath Krishnan, Acta Physica Polonica A, 125 (2014) 18-22.

[58] G. Keresztury, G. Jalsovszky, J. Mol. Struct. 10 (1971) 304-305.

[59] A.P. Scott, L. Random, J. Phys Chem. 100 (1996) 16502-16513.

[60] NIST Computational Chemistry Comparison and Benchmark Database NIST Standard Reference Database, Number 101 Release 16a (2013), (Eds) D. R. Johnson III http://cccbdb.nist.gov/.

[61] M. Alcolea Palafox, Int. J. Quantum Chem. 77 (2000) 661-684.

[62] M. Alcolea Palafox, V.R. Rastogi, Spectrochim. Acta A58 (2002) 411-440.

[63] Th. Zeegers-Huyskens, Spectrochim. Acta A 23 (1967) 855-866.

[64] A.W. Baker, H.O. Kerlinger, A.T. Shulgin, Spectrochim. Acta 20 (1964) 1477-1486.

[65] B. Schrader (Ed), Infrared and Raman Spectroscopy. Model and Applications, VCH, Weinheim, 1995.

[66] W.F. Maddams, M.J. Southon, Spectrochim. Acta 38A (1992) 459-466.

[67] G. Talsky, Derivative Spectroscopy, VCH, Weinheim, 1994.

[68] E. Pretsch, P. Bühlmann, C. Affolter, Structure Determination of Organic Compounds, Springer, Berlin-Verlag, 2000.

[69] The Handbook of Infrared and Raman Characteristic Frequencies of Organic Compounds, D. Lin-Vien, N.B. Colthup, W.G. Fateley, J.G. Grosselii, Academic Press, San Diego, 1991.

[70] Gauss View 3.0, Gaussian Inc, Pittsburg, PA 15106, USA, 2000-2003 Semichem. Inc.

[71] A. Katrusiak, J. Mol. Graph. Modelling, 19 (2001) 363-367.

FIGURE CAPTIONS

Fig. 1. The centrosymmetric dimer ,2:2 complex of (*R*) and (*S*) piperidinium-3-carboxylic acid 2,6-dichloro-4-nitrophenolates, $R^4_4(28)$. Hydrogen bonds are indicated as cyan lines.

Fig. 2. (a) The 4:4 complex (cyclamer) of two (*R*)- and two (*S*)-piperidinium-3-carboxylic acid 2,6-dichloro-4-nitrophenolates linked by O-H···O, N-H···O and C-H···Cl hydrogen bonds indicated by cyan lines, $R^4_4(28)$-$R^4_4(20)$-$R^4_4(28)$ cyclamer; (b) the same as a stereo projection [71] along the [010] direction.

Fig. 3. Structures of complexes of piperidne-3-carboxylic acid with 2,6-dichloro-4-nitrophenol: 1:1, **2-M*a*** and **2-M*b***; 2:2, **2-D,** optimized by the B3LYP/6-311++G(d,p) and 4:4, **2-C**, by the B3LYP/6-31G(d,p) approach. The numbers (I) and (II) describe the molecules in complex of the stoichiometry 2:2, **2-D** and (I) – (IV) in the complex in the stoichiometry 4:4, **2-C**.

Fig. 4. Spectra of piperidinium-3-carboxylic acid 2,6-dichloro-4-nitrophenolate (a) Raman (**1**), (b) the second derivative IR spectrum (**1**), (c) the solid-state FTIR of **1,** solid black line; of piperidine-3-carboxylic acid, long dashed red line; of 2,6-dichloro-4-nitrophenol, short dashed blue line; Black wavenumbers describing the bands in the spectrum of **1,** and (d) the IR spectrum of **D-2** calculated by the B3LYP/6-311++G(d,p) approach and all wavenumbers scaled by 0.967.

Fig. 5. The infrared spectra of complexes of piperidine-3-carboxylic acid with 2,6-dichloro-4-nitrophenol (a) 1:1, **2-M*a***, (b) 1:1, **2-M*b***, (c) 2:2, **2-D** of calculated by the B3LYP/6-311++G(d,p) approach and all wavenumbers scaled by 0.967, and (d) 4:4, **2-C** calculated by the B3LYP/6-31G(d,p) approach and all wavenumbers scaled by 0.961.

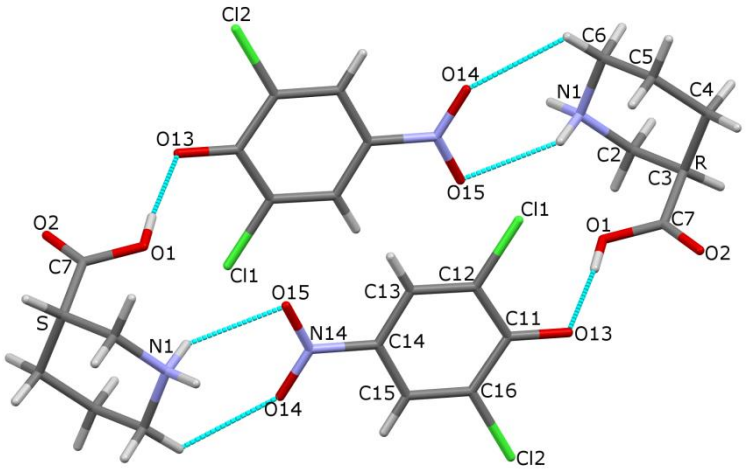

Fig. 1.

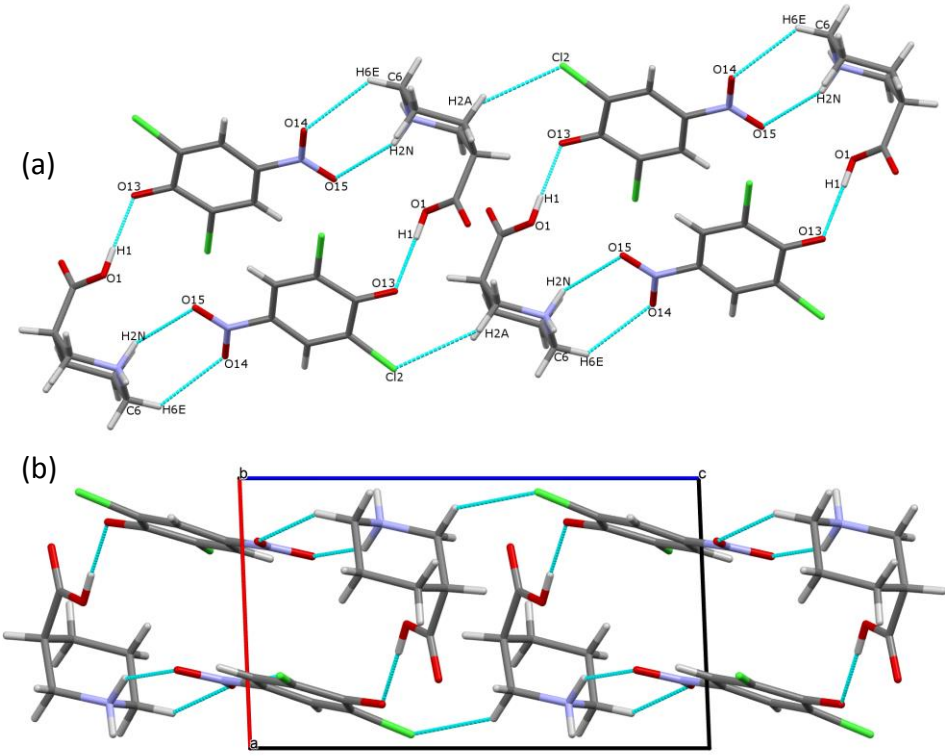

Fig. 2.

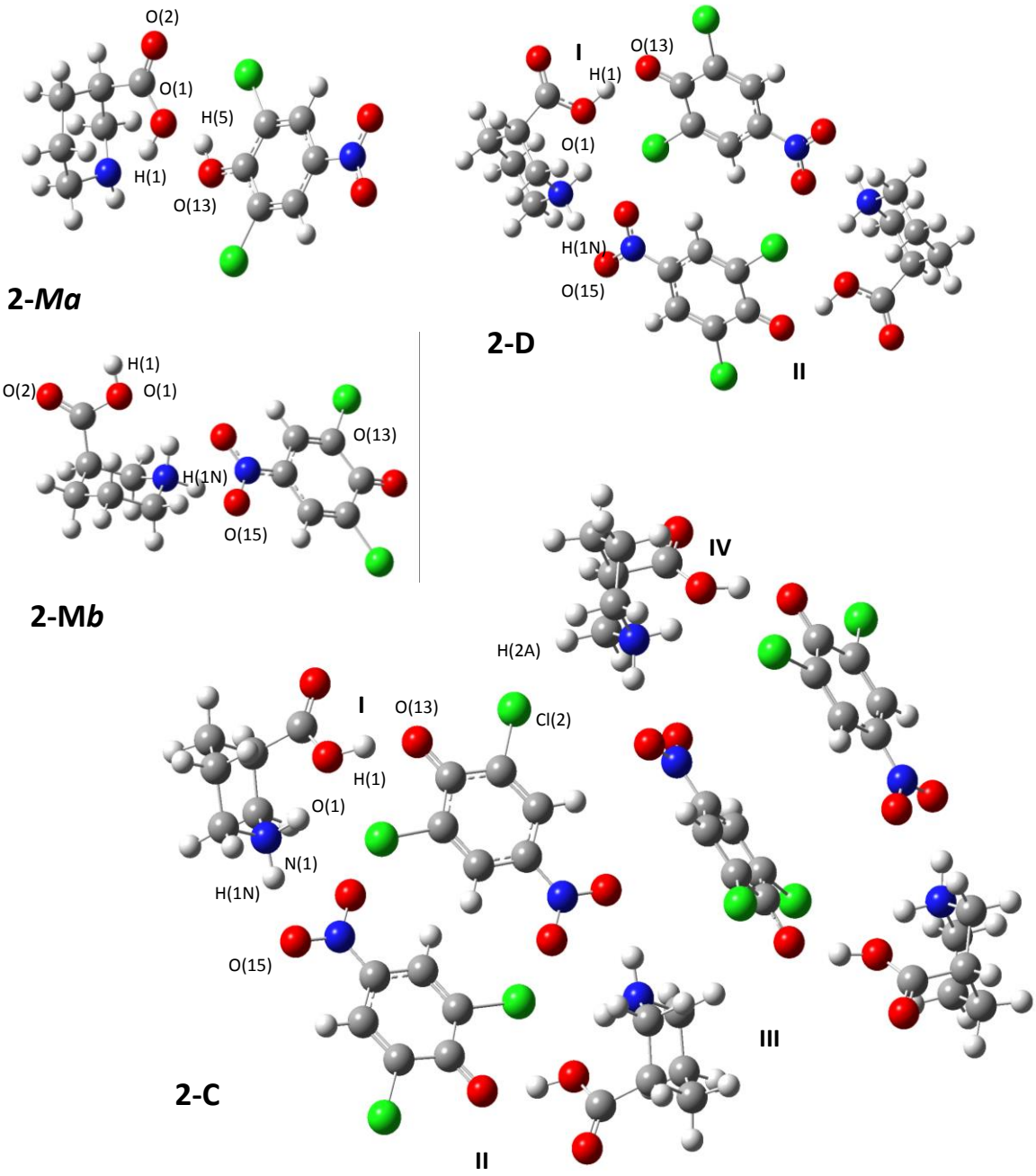

Fig. 3.

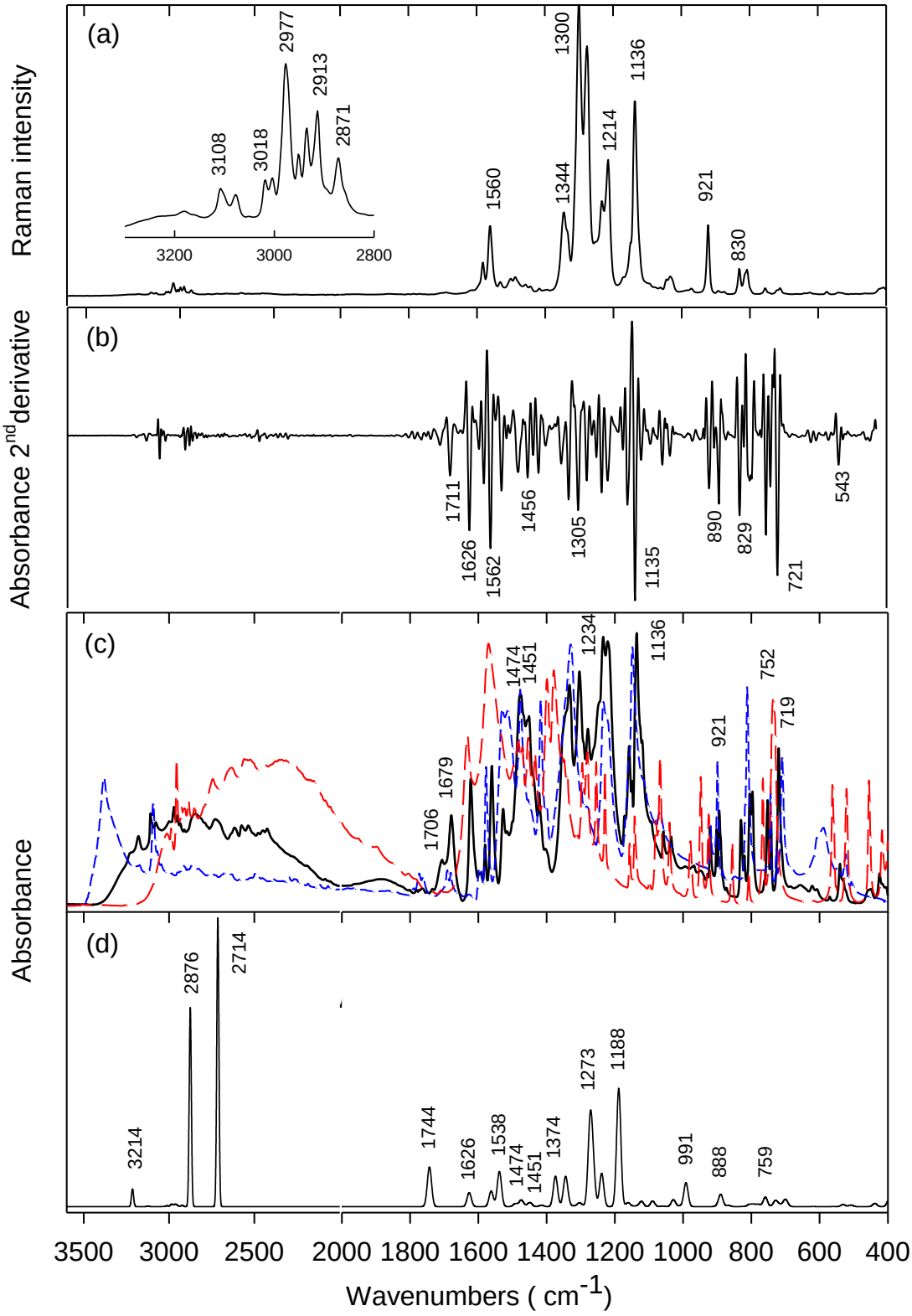

Fig. 4

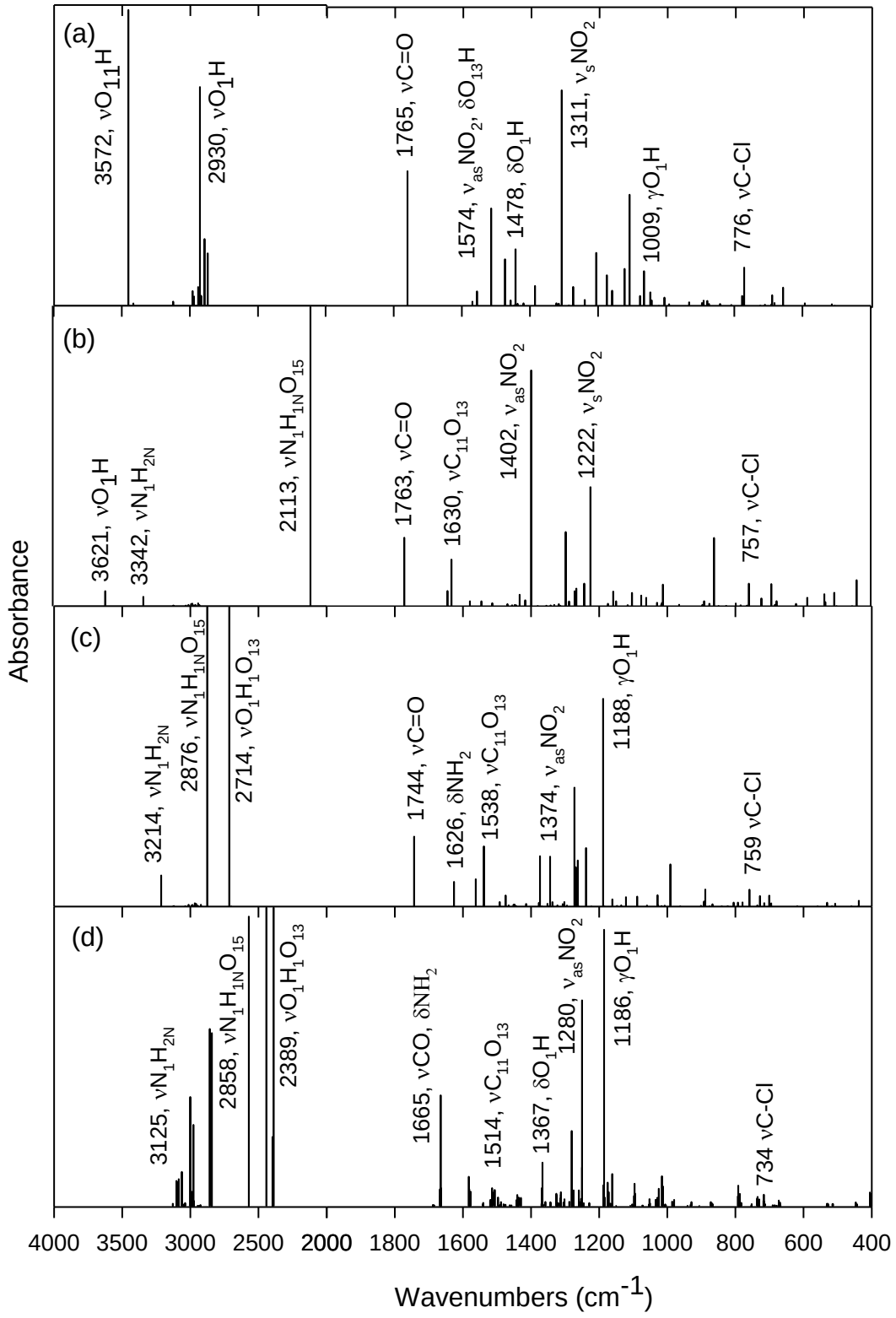

Fig. 5.

Table 1

Crystal data and structure refinement for piperidinium-3-carboxylic acid 2,6-dichloro-4-nitrophenolate.

Empirical formula	$C_{12}H_{14}Cl_2N_2O_5$
Formula weight	337.15
Temperature	293(2) K
Wavelength	0.71073 Å
Crystal system	Triclinic
Space group	$P\bar{1}$
Unit cell dimensions.	a = 6.9793(4) Å
	b = 8.9563(7) Å
	c = 12.2457(9) Å
	α = 73.358(7)°
	β = 85.424(5)°
	γ = 81.553(5)°
Volume	724.87(9) Å^3
Z	2
Calculated density	1.545 g/cm^3
Absorption coefficient	0.470 mm^{-1}
F(000)	348
Crystal size	0.54 x 0.32 x 0.10 mm
θ range for data collection	3.33 to 25.38°
Limiting indices	$-8 \le h \le 8$, $-10 \le k \le 10$, $-14 \le l \le 14$
Reflections collected / unique	11146 / 2432 [R(int) = 0.0434]
Completeness to θ= 25.38	90.6 %

Absorption correction	None
Refinement method	Full-matrix least-squares on F^2
Data / restraints / parameters	2432 / 0 / 190
Goodness-of-fit on F^2	0.989
Final R indices [I>2σ(I)]	R1 = 0.0538, wR2 = 0.1328
R indices (all data)	R1 = 0.0661, wR2 = 0.1414
Largest diff. peak and hole	0.373 and -0.270 $eÅ^{-3}$

Table 2

Selected experimental and calculated, by the B3LYP/6-311++G(d,p) approach, bond lengths (Å), bond and torsion angles (°) for the complex of piperidine-3-carboxylic acid with 2,6-dichloro-4-nitrophenol[a] .

	X-Ray	*B3LYP*						
	1	**2-M*a***	**2-M*b***	**2-D**(I,II)	**2-C**(I)	**2-C**(II)	**2-C**(III)	**2-C**(IV)
Bond lengths								
N(1)-C(2)	1.489(4)	1.475	1.495	1.502	1.516	1.514	1.514	1.516
C(2)-C(3)	1.525(4)	1.539	1.534	1.534	1.539	1.539	1.539	1.539
C(3)-C(4)	1.528(4)	1.551	1.551	1.548	1.552	1.558	1.558	1.558
C(4)-C(5)	1.518(5)	1.537	1.535	1.536	1.543	1.543	1.544	1.543
C(5)-C(6)	1.509(4)	1.532	1.528	1.528	1.534	1.535	1.535	1.534
N(1)-C(6)	1.478(4)	1.477	1.494	1.499	1.513	1.510	1.510	1.516
C(3)-C(7)	1.508(4)	1.534	1.523	1.537	1.531	1.532	1.532	1.530
C(7)-O(1)	1.309(4)	1.355	1.364	1.336	1.365	1.362	1.361	1.364
C(7)-O(2)	1.201(4)	1.202	1.200	1.204	1.231	1.233	1.233	1.232
C(11)-C(12)	1.418(4)	1.410	1.478	1.454	1.449	1.443	1.445	1.450
C(12)-C(13)	1.382(4)	1.383	1.356	1.366	1.367	1.370	1.368	1.367
C(13)-C(14)	1.381(5)	1.391	1.425	1.410	1.416	1.413	1.414	1.416
C(14)-C(15)	1.378(5)	1.390	1.425	1.412	1.418	1.412	1.415	1.418

C(15)-C(16)	1.372(4)	1.384	1.356	1.366	1.368	1.370	1.370	1.368
C(11)-C(16)	1.410(4)	1.409	1.478	1.455	1.452	1.443	1.446	1.452
C(11)-O(13)	1.290(3)	1.333	1.223	1.251	1.277	1.289	1.282	1.277
C(12)-Cl(1)	1.727(3)	1.747	1.748	1.761	1.825	1.824	1.825	1.824
C(14)-N(14)	1.455(4)	1.470	1.364	1.399	1.393	1.403	1.405	1.393
N(14)-O(14)	1.224(4)	1.226	1.261	1.245	1.308	1.301	1.299	1.308
N(14)-O(15)	1.229(4)	1.226	1.300	1.268	1.287	1.279	1.282	1.287
C(16)-Cl(2)	1.738(3)	1.742	1.747	1.747	1.809	1.818	1.820	1.810

Bond angles

N(1)-C(2)-C(3)	111.1(2)	108.56	122.55	110.85	109.67	109.91	109.80	109.89
C(2)-C(3)-C(4)	110.4(2)	109.18	110.53	110.14	109.99	110.03	109.95	110.03
C(3)-C(4)-C(5)	111.3(3)	112.42	112.17	112.04	112.31	112.23	112.36	112.91
C(4)-C(5)-C(6)	111.4(3)	111.43	111.44	111.70	111.84	111.77	111.80	111.65
C(5)-C(6)-N(1)	109.9(2)	109.70	111.36	110.64	110.02	110.16	110.07	109.99
C(6)-N(1)-C(2)	112.6(2)	112.01	113.58	113.18	112.79	112.86	112.73	112.56
C(2)-C(3)-C(7)	114.2(3)	113.11	114.73	113.64	112.72	112.62	112.51	112.83
C(4)-C(3)-C(7)	110.3(3)	110.81	110.47	110.55	111.25	111.13	111.27	111.10
C(3)-C(7)-O(1)	113.9(2)	115.76	112.88	111.37	111.62	111.75	111.66	111.61
C(3)-C(7)-O(2)	123.0(3)	123.03	124.67	122.83	123.66	123.44	123.34	123.65

O(1)-C(7)-O(2)	123.1(3)	121.20	122.44	125.78	124.74	124.77	124.96	124.70
C(11)-C(12)-C(13)	122.8(3)	121.65	123.65	123.80	124.25	124.07	124.15	124.20
C(12)-C(13)-C(14)	118.4(3)	118.67	119.56	119.08	118.82	118.68	119.00	118.87
C(13)-C(14)-C(15)	122.1(3)	121.92	120.48	120.74	120.57	120.89	120.69	120.55
C(14)-C(15)-C(16)	118.1(3)	118.50	119.61	113.36	119.06	118.62	118.32	119.04
C(15)-C(16)-C(11)	123.8(3)	121.81	123.60	123.38	123.87	124.17	124.71	123.90
C(16)-C(11)-C(12)	114.7(3)	117.46	113.10	113.56	113.39	113.55	113.06	113.38
C(12)-C(11)-O(13)	122.8(3)	118.40	123.46	124.19	124.56	124.48	124.95	124.56
C(16)-C(11)-O(13)	122.5(3)	124.14	123.44	122.24	122.05	121.94	121.99	122.06
C(11)-C(12)-Cl(1)	118.0(2)	118.79	116.39	117.50	117.49	117.51	117.59	117.51
C(13)-C(12)-Cl(1)	119.2(3)	119.60	120.25	118.70	118.26	118.40	118.25	118.29
C(13)-C(14)-N(14)	118.8(3)	119.04	120.24	119.04	119.06	119.22	118.69	119.08
C(15)-C(14)-N(14)	119.0(3)	119.04	119.28	120.20	120.36	119.90	120.62	120.36
C(14)-N(14)-O(14)	118.5(3)	117.69	122.24	120.56	119.39	118.98	119.58	119.37
C(14)-N(14)-O(15)	118.2(3)	117.69	119.26	119.13	120.62	120.37	119.94	120.58
O(14)-N(14)-O(15)	123.3(3)	124.62	118.51	120.30	119.98	120.63	120.47	120.04
C(11)-C(16)-Cl(2)	117.1(2)	118.13	116.31	116.83	116.81	116.98	115.90	116.81
C(15)-C(16)-Cl(2)	119.1(3)	120.06	120.09	119.77	119.32	118.84	119.37	119.28

Torsion angles

N(1)-C(2)-C(3)-C(4)	-53.8(3)	-58.53	-51.73	-54.93	-56.39	56.07	-56.25	56.17
C(2)-C(3)-C(4)-C(5)	53.0(3)	52.33	51.67	53.29	53.53	-53.49	53.24	-53.62
C(3)-C(4)-C(5)-C(6)	-55.0(4)	-49.87	-53.21	-52.92	-52.23	52.39	-52.06	52.90
C(4)-C(5)-C(6)-N(1)	56.7(4)	53.01	53.93	53.37	53.20	-53.32	53.26	-53.90
C(5)-C(6)-N(1)-C(2)	-58.4(3)	-62.14	-54.99	-56.59	-58.25	57.98	-58.40	58.41
C(6)-N(1)-C(2)-C(3)	57.6(3)	65.36	54.48	57.94	60.39	-59.91	60.48	-60.08
N(1)-C(2)-C(3)-C(7)	71.2(3)	65.35	74.06	69.73	66.39	-68.51	68.38	-68.52
C(5)-C(4)-C(3)-C(7)	-74.1(3)	-72.89	-76.48	-73.13	-72.08	71.95	-72.09	72.07
C(2)-C(3)-C(7)-O(1)	-6.3(4)	-34.18	-30.00	-28.90	-36.08	35.34	-37.72	36.87
C(4)-C(3)-C(7)-O(1)	118.7(3)	88.85	95.87	95.53	88.01	-88.64	86.17	-87.24
C(2)-C(3)-C(7)-O(2)	172.3(3)	147.18	151.53	153.01	145.98	-146.95	144.29	-145.34
C(4)-C(3)-C(7)-O(2)	-62.6(4)	-34.12	82.60	-82.55	-89.93	89.08	-91.81	90.55
C(11)-C(12)-C(13)-C(14)	-0.2(4)	0.03	-0.03	-0.38	0.48	-0.14	0.45	-0.46
C(12)-C(13)-C(14)-C(15)	2.7(4)	0.13	-0.04	-1.52	1.42	0.94	1.38	-1.37
C(13)-C(14)-C(15)-C(16)	-1.7(4)	-0.03	0.09	1.02	-1.18	-0.34	-1.27	1.12
C(14)-C(15)-C(16)-C(11)	-2.0(4)	-0.23	-0.06	1.42	-0.97	-1.10	-0.67	1.00
C(15)-C(16)-C(11)-C(12)	4.2(4)	0.37	-0.01	-3.05	2.61	1.77	2.27	-2.59
C(16)-C(11)-C(12)-C(13)	-3.0(4)	-0.26	0.06	2.53	-2.36	-1.13	-2.15	2.32
C(14)-C(13)-C(12)-Cl(1)	-178.4(2)	179.99	179.96	179.33	-178.98	178.02	-178.98	178.98

C(16)-C(11)-C(12)-Cl(1)	175.2(2)	179.77	-179.94	-177.19	177.09	-179.30	177.29	-177.13
C(12)-C(11)-C(16)-Cl(2)	-173.9(2)	-179.39	179.99	178.56	-178.72	-177.65	-179.13	178.71
C(14)-C(15)-C(16)-Cl(2)	176.1(2)	179.52	179.94	179.76	-179.60	178.32	-179.23	179.67
O(13)-C(11)-C(12)-C(13)	178.1(3)	179.92	-179.93	-177.34	177.77	176.91	178.31	-177.85
O(13)-C(11)-C(16)-C(15)	-176.9(3)	-179.83	179.98	176.84	-177.52	-176.33	-178.17	177.58
O(13)-C(11)-C(12)-Cl(1)	-3.7(4)	-0.05	0.07	2.92	-2.78	-1.26	-2.26	2.70
O(13)-C(11)-C(16)-Cl(2)	5.0(4)	0.42	-0.02	-1.55	1.15	4.25	0.43	-1.13
C(12)-C(13)-C(14)-N(14)	178.4(3)	-179.92	179.79	176.75	-177.55	-179.34	-177.56	177.51
C(16)-C(15)-C(14)-N(14)	-177.4(3)	-179.99	-179.75	-177.23	177.78	179.94	177.65	-177.76
C(13)-C(14)-N(14)-O(14)	177.0(3)	179.72	179.95	1.40	179.28	176.41	177.24	-179.16
C(15)-C(14)-N(14)-O(14)	-7.2(4)	-0.32	-0.22	179.68	0.31	-3.86	-1.71	-0.27
C(13)-C(14)-N(14)-O(15)	-2.8(4)	-0.27	-0.16	-177.35	0.28	-4.09	-1.81	-0.14
C(15)-C(14)-N(14)-O(15)	173.0(3)	179.69	179.67	0.93	-178.73	175.64	179.24	178.75

[a] (see Figs. 1 and 3). Numbers I, II, III and IV denote the $P3C^{+}H{\cdot}DCNP^{-}$ units joined into 2:2 (**2-D**) and 4:4 (**2-C**) complexes.

Table 3.

Geometry of the O-H···O and N-H···O hydrogen bonds, the C-H···Cl and C-H···O contacts for the complex of piperidine-3-carboxylic acid with 2,6-dichloro-4-nitrophenol (Å and °).

	D-H···A[a]	D-H	H···D	D···A	∠DHA
X-ray					
1	O(1)-H(1)···O(13)	0.82	1.75	2.57(1)	172
	N(1)-H(1N)···O(13)[b]	0.90	1.83	2.73(1)	171
	N(1)-H(2N)···O(15)[c]	0.90	2.31	3.06(1)	141
	C(2)-H(2A)···Cl(2)[d]	0.97	2.90	3.71(1)	141
	C(6)-H(6A)···O(2)[b]	0.97	2.65	3.42(1)	137
	C(6)-H(6E)···O(14)[c]	0.97	2.38	3.27(1)	127
B3LYP					
2-M*a*	O(1)-H(1)···N(1)	1.004	1.738	2.668	152.1
	O(13)-H(5)···O(1)	0.978	1.934	2.761	140.6
2-M*b*	N(1)-H(2N)···O(15)	1.100	1.501	2.600	178.1
2-D	$O(1_I)$-$H(1_I)$···$O(13_I)$	1.021	1.545	2.541	163.7
	$N(1_I)$-$H(2N_I)$···$O(15_{II})$	1.049	1.731	2.773	171.1
	$O(1_{II})$-$H(1_{II})$···$O(13_{II})$	1.021	1.454	2.541	163.7
	$N(1_{II})$-$H(2N_{II})$···$O(15_I)$	1.049	1.731	2.773	171.1
2-C	$O(1_I)$-$H(1_I)$···$O(13_I)$	1.053	1.448	2.490	169.5
	$N(1_I)$-$H(2N_I)$···$O(15_{II})$	1.051	1.726	2.769	170.6
	$O(1_{II})$-$H(1_{II})$···$O(13_{II})$	1.038	1.494	2.521	168.9
	$N(1_{II})$-$H(2N_{II})$···$O(15_I)$	1.041	1.868	2.889	165.9
	$C(2_{II})$-$H(2_{II})$···$Cl(2_{III})$	1.093	2.996	3.861	136.3
	$O(1_{III})$-$H(1_{III})$···$O(13_{III})$	1.049	1.461	2.496	167.8
	$N(1_{III})$-$H(2N_{III})$···$O(15_{IV})$	1.051	1.730	2.773	170.8

$O(1_{IV})$-$H(1_{IV})\cdots O(13_{IV})$	1.040	1.488	2.514	168.7
$N(1_{IV})$-$H(2N_{IV})\cdots O(15_{III})$	1.043	1.788	2.819	164.8
$C(2_{IV})$-$H(2_{IV})\cdots Cl(2_{I})$	1.093	2.966	3.801	133.4

[a] Letters A and E denote the axial or equatorial positions of the hydrogen atom; numbers I, II, III and IV denote $P3C^{+}H{\cdot}DCNP^{-}$ units joined into 2:2 (**2-D**) and 4:4 (**2-C**) complexes.
Symmetry codes: [b] -1+x, y, z; [c] 1-x, 2-y, -z; [d] 1-x, 1-y, 1-z.

Table 4.

Selected natural atomic charges (NBO) (*e*) in the complexes of piperidine-3-carboxylic acid with 2,6-dichloro-4-nitrophenol. 1:1 (**2-M*a*, 2-M*b***), 2:2 (**2-D**),piperidine-3-carboxylic acid (P3C), and 2,6-dichloro-4-nitrophenol (DCNP).

Atom[a]	**2-M*a***	**2-M*b***	**2-D** (I)	**2-D** (II)	**P3C**	**DCNP**
N(1)	-0.7104	-0.6025	-0.6068	-0.6068	-0.7116	-
C(2)	-0.1840	-0.1810	-0.1728	-0.1728	-0.1852	-
C(3)	-0.3286	-0.3315	-0.3287	-0.3287	-0.3285	-
C(4)	-0.3759	-0.3750	-0.3767	-0.3767	-0.3765	-
C(5)	-0.3035	-0.4091	-0.4116	-0.4116	-0.4021	-
C(6)	-0.1742	-0.1714	-0.1670	-0.1670	-0.1737	-
C(7)	0.8081	0.8115	0.8110	0.8110	0.8019	-
O(1)	-0.7558	-0.7211	-0.7644	-0.7645	-0.7127	-
O(2)	-0.5775	-0.5697	-0.5808	-0.5807	-0.5915	-
H(1)	0.5032	0.4995	0.5342	0.5342	0.4971	-
C(11)	0.3080	0.4077	0.4007	0.4007	-	0.2986
C(12)	-0.0744	-0.0972	-0.1024	-0.1025	-	-0.0731
C(13)	-0.1977	-0.2080	-0.1903	-0.1903	-	-0.1918
C(14)	0.0634	0.0633	0.0403	0.0403	-	0.0694
C(15)	-0.1970	-0.2079	-0.1936	-0.1936	-	-0.1971
C(16)	-0.0944	-0.0958	-0.0984	-0.0984	-	-0.0890
O(13)	-0.6637	-0.5593	-0.6789	-0.6789	-	-0.6365
N(14)	0.4855	0.4227	0.4615	0.4615	-	0.4861
O(14)	-0.3833	-0.5293	-0.4640	-0.4640	-	-0.3776
O(15)	-0.3835	-0.5805	-0.5213	-0.5213	-	-0.3744
Cl(1)	0.0373	0.0218	-0.0139	-0.0139	-	0.0550

Cl(2)	0.0446	0.0234	0.0290	0.0290	-	0.0202
H(1N)	0.3558	0.4645	0.4570	0.4570	0.3683	-
H(2N)	-	0.4261	0.4568	0.4568	-	-
H(5)	0.5204	-	-	-	-	0.4876

[a] For number of atom see Figs 1 and S2 (supplementary material).

Table 5.

Selected frequencies for piperidinium-3-carboxylic acid 2,6-dichloro-4-nitrophenolate (ν, cm^{-1}) observed for **1**, calculated and scaled for **2-D** (B3LYP/6-311++G(d,p).

1	**1**	**1**	**2-D**				
Raman	**FTIR**	d^2	IR				
ν_{exp}[a]	ν_{exp}[a]	νd^2 [b]	ν_{calc}	A[c]	ν_{scaled}[d]	S_n[e], PED[f] (%)	Assignments[g]
	3223 w		3324	413	3214	S_1 (98)	νNH
	3179 m	3179	3323	4	3213	S_3 (98)	νNH
			3231	5	3124	S_9 (94)	νCH^{Ar}
3108 vw	3109 m	3108	3227	6	3121	S_8 (82), S_{10} (18)	νCH^{Ar}
3077 vw	3078 m	3079	3141	3	3037	S_{16} (14), S_{17} (80)	$\nu_{as}CH_2$
3018 vw			3116	24	3013	S_{15} (83)	$\nu_{as}CH_2$
3004 vw	3000 m	3000	3093	15	2991	S_{12} (76), S_{18} (11)	$\nu_{as}CH_2$
			3093	11	2991	S_{21} (76), S_{27} (12)	$\nu_{as}CH_2$
			3087	21	2985	S_{21} (12), S_{27} (65)	$\nu_{as}CH_2$
			3087	9	2985	S_{12} (12), S_{18} (65)	$\nu_{as}CH_2$
			3083	10	2981	S_{20} (83)	νCH^{Pip}
			3083	8	2981	S_{11} (83)	νCH^{Pip}
2977 vw	2971 m	2973	3069	44	2968	S_{16} (72), S_{17} (13)	ν_sCH_2
2951 vw	2950 w	2950	3059	36	2958	S_{14} (76)	ν_sCH_2
2935 vw	2934 w	2934	3047	10	2946	S_{28} (91)	ν_sCH_2
			3047	10	2946	S_{19} (91)	ν_sCH_2
			3023	23	2923	S_{13} (78), S_{22} (11)	ν_sCH_2
2913 vw	2910 w	2910	3023	14	2923	S_{13} (11), S_{22} (78)	ν_sCH_2
2871 vw	2853 m		2974	4654	2876	S_5 (97)	νNH···O
			2972	2	2874	S_6 (93)	νNH···O
	2570 m		2807	6763	2714	S_2 (81)	νOH···O
	1706 w	1711	1803	930	1744	S_{32} (84)	$\nu_{as}COO$
	1679 m	1662	1682	328	1626	S_{79} (19), S_{81} (40)	δNH_2, δCNH

1851 w	1622 m	1626	1616	364	1563	S_{40} (55), S_{86} (13)	νCC^{Ar}, δCCH^{Ar}
1560 m	1561 s	1562	1591	22	1538	S_{34} (65), S_{35} (11)	$\nu C\text{-}O^{Ar}$
1530 vw	1527 m	1531	1591	800	1538	S_{34} (11), S_{35} (66)	$\nu C\text{-}O^{Ar}$
		1516	1543	11	1492	S_{44} (39)	νCC^{Ar}
1500 w	1479 s	1503	1543	61	1492	S_{38} (35)	νCC^{Ar}, νNO
1487 vw	1474 s	1480	1525	148	1474	S_{138} (11), S_{139} (15)	δNH_2
1456 vw	1456 s	1456	1516	16	1466	S_{101} (65), S_{160} (11)	δCH_2
			1516	9	1466	S_{96} (67)	δCH_2
1442 vw	1451 m	1439	1501	22	1451	S_{39} (26) S_{94} (11)	νCC^{Ar}, δCH_2
			1498	25	1449	S_{94} (48)	δCH_2
			1494	3	1445	S_{105} (68)	δCH_2
			1494	8	1445	S_{98} (68)	δCCH^{Pip}
1416 vw	1421 m	1421	1463	35	1415	S_{71} (16), S_{139} (11)	δOH, δNH_2
			1424	50	1377	S_{94} (15), S_{160} (19), S_{161} (15)	δCH_2, δCCH^{Pip}
1394 vw	1376 w	1401	1421	670	1374	S_{43} (52)	νNO
		1355	1398	35	1352	S_{101} (15), S_{154} (10)	δCH_2, $\tau NCCH^{Pip}$
			1390	664	1344	S_{68} (18), S_{86} (28)	νCN^{Ar}, νNO, δCCH^{Ar}
1344 m	1333 vs	1334	1383	57	1337	S_{152} (11)	$\tau CCCH^{Pip}$
			1368	15	1323	S_{148} (16), S_{156} (15)	$\tau CCCH^{Pip}$, $\tau OCCH$
			1352	32	1308	S_{93} (12), S_{153} (36)	δCCH^{Pip}, $\tau CCCH^{Pip}$
1300 vs	1303 vs	1305	1347	60	1303	S_{70} (11)	δCNH^{Pip}
			1339	14	1295	S_{88} (24)	δCCH^{Pip}
1276 vs	1279 s	1278	1316	1582	1273	S_{68} (17), S_{88} (10)	νCN^{Ar}, νNO, δCCH^{Pip}
		1261	1312	524	1269	S_{156} (14)	$\tau OCCH^{Pip}$
		1253	1306	613	1263	S_{68} (11), S_{87} (23)	νCN^{Ar}, νNO, δCCH^{Ar}
1233 m	1234 vs	1235	1281	780	1239	S_{88} (26)	δCCH^{Pip}
1214 m	1220 vs	1220	1229	2765	1188	S_{48} (28)	νCO^{Pip}
		1159	1201	96	1161	S_{155} (17)	$\tau NCCH^{Pip}$
			1186	8	1149	S_{93} (13), S_{160} (17)	δCCH^{Pip}, $\tau CCCH^{Pip}$

1136 s	1136 vs	1135	1174	15	1135	S_{87} (45)	δCCH^{Ar}
	1119 s	1121	1160	126	1122	S_{51} (42)	νCC^{Ar}, νCN^{Ar}, νNO, νCCl
	1093 w	1098	1126	133	1089	S_{48} (12), S_{88} (15), S_{93} (12)	νCO^{Pip}, δCCH^{Pip}
	1058 w	1061	1096	14	1060	S_{57} (25), S_{58} (16)	νCC^{Pip}, νCN^{Pip}
1033 vw	1034 w	1036	1064	151	1029	S_{69} (12), S_{73} (13), S_{85} (29), S_{115} (10)	νCCl, δCCH^{Ar}, δCCC^{Ar}
			1061	13	1026	S_{74} (13), S_{86} (22), S_{117} (12)	δCCC^{Ar}, δCCH^{Ar}
			1042	12	1008	S_{58} (11), S_{63} (10), S_{64} (30)	νCC^{Pip}, νCN^{Pip}
921 m	921 m	921	1025	561	991	S_{168} (33), S_{183} (11)	γOH
			995	1	962	S_{102} (10), S_{187} (12)	δCCH^{Pip}, $\tau CCCN^{Pip}$
	902 m	910	932	9	901	S_{159} (12)	$\tau CCCH^{Pip}$
	894 m		923	68	893	S_{146} (79)	$\tau NCCH^{Ar}$
	873 vw	890	919	227	888	S_{45} (58)	νCC^{Ar}, νNO, νCCl
			897	31	867	S_{125} (12)	δCCN^{Pip}
830 w	830 m	829	869	2	840	S_{54} (11), S_{57} (44)	νCC^{Pip}, νCN^{Pip}
	820 w	820	851	5	823	S_{63} (15)	νCC^{Pip}, νCN^{Pip}
808 w	805 m	797	833	53	806	S_{112} (16), S_{113} (23)	δCCC^{Ar}, δONO
	797 m	797	820	53	793	S_{62} (31)	νCC^{Pip}, νCN^{Pip}
			806	55	779	S_{58} (10), S_{63} (26), S_{193} (11)	νCC^{Pip}, νCN^{Pip}, $\gamma OCOC$
754 vw	752 m	750	785	224	759	S_{66} (53), S_{117} (18)	δCCl, δCCC^{Ar}
	742 m	742	761	15	736	S_{72} (12), S_{171} (12), S_{180} (15), S_{200} (14), S_{203} (11)	δOCH^{Ar}, $\tau CCCC^{Ar}$, $\gamma CCCCl$
			753	139	728	S_{108} (17), S_{193} (27)	δOCO, $\gamma OCOC$
710 vw	719 s	721	740	45	716	S_{194} (80)	γNO_2
			725	145	701	S_{114} (42)	δONO
623 vw	622 vw	625	719	42	695	S_{193} (21)	$\gamma OCOC$
			640	2	619	S_{123} (25)	δCCN^{Ar}
541 wv	540 w	543	578	3	559	S_{56} (23), S_{109} (22)	νCC^{Pip}, δOCO
	534 w	525	549	52	531	S_{117} (10)	δCCC^{Ar}

		534	3	516	S_{178} (10), S_{203} (10), S_{204} (52)	$\gamma CCNC^{Ar}$, $\tau CCCC^{Ar}$, $\gamma CCCO^{Ar}$, $\gamma CCNC^{Ar}$
		525	38	508	S_{125} (30)	δCCN^{Pip}
457 vw	465	475	1	459	S_{143} (10), S_{172} (18), S_{197} (47)	$\tau NCCH^{Ar}$, $\tau CCCH^{Ar}$, $\tau CCCC^{Ar}$, $\gamma CCCCl$
451 vw	447	453	77	438	S_{126} (10)	δCCC^{Pip}
424 vw		410	163	396	S_{108} (12)	δOCO

[a] vs – very strong, s – strong, m – medium, w – weak, vw – very weak,

[b] d^2 – second derivative,

[c] A_{calc} – intensity in $km \cdot mol^{-1}$,

[d] Scaling factor: 0.967,

[e] S_n - symmetry coordinate (for details see Table S2 in supplementary information),.

[f] PED – the potential energy distribution, % in brackets,

[g] ν – stretching; δ – in-plane deformation; γ – out-of-plane deformation; τ – torsion; Ar – phenyl ring; Pip – piperidinium ring.